

DESIGN OF A PHOTONIC CRYSTAL ACCELERATOR FOR BASIC RADIATION BIOLOGY*

A. Aimidula[#], C.P. Welsch, Cockcroft Institute and The University of Liverpool, UK
 G. Xia, The University of Manchester, UK
 K. Koyama, Y. Matsumura, M. Uesaka, The University of Tokyo, Japan
 T. Natsui, M. Yoshida, High Energy Accelerator Research Organization (KEK), Japan

Abstract

The application of photonic crystals to realize an on-chip electron beam source for fundamental radiation biology is highly interesting for a number of applications. The unique combination of nanometre beam size and attosecond-short pulses has a very promising potential for use in microscopic and ultra-fast analyses of the damage and repair of radiation-irradiated DNA and chromosomes. Simulation studies indicate an output electron beam energy, beam intensity and device size of the order of MeVs, fCs and a few cm, respectively.

In this contribution, first results from numerical studies into the design of such compact accelerator structures are presented. The dimensions of a novel dual-grating-based acceleration structure are shown together with the estimated laser parameters. Finally, a system consisting of an electron injector and multi-stage accelerating structures is proposed, which corresponds to a miniaturized optical linear accelerator.

INTRODUCTION

Since the transverse dimensions of the acceleration cavity of Photonic Crystal Accelerators (PCA) are on the operating laser wavelength scale, they are able to deliver nm-beams of sub-fs pulses. These high quality beams have a unique advantage for investigating the basic radiobiology process as they are able to target a single DNA strand [1]. There are currently three candidates for photonic crystal accelerator structures: the dual-grating structure, photonic crystal fibres and the woodpile structure [2, 3, 4]. The development of nano technology has enabled more precise fabrication of these structures at lower cost. SLAC demonstrated that very high acceleration gradients can be achieved in their latest experiment [5]. In this paper, we introduce and analyse a new dual-grating structure based on the original idea from Plettner [2] but with the position of pillars slightly changed. The basic working principle of dual-grating structures is based on decreasing the phase velocity of the electric field, thereby synchronizing it with non-relativistic and relativistic electrons. We show that this structure can also efficiently modify the laser field.

* This work is supported by the EU under Grant Agreement 289191, the STFC Cockcroft Institute core grant No. ST/G008248/1, and by KAKENHI, Grant-in-Aid for Scientific Research (C) 24510120.
[#] aimidula.aimierding@liverpool.ac.uk

DIMENSIONS AND FIELD DISTRIBUTION

The proposed structure cross section geometry and dimensions are shown in Fig. 1. The lattice length L is λ , the dielectric length D and vacuum length are both equal to $\lambda/2$, where λ is the wavelength of the operating laser. Driving laser light is fed from the two outer surfaces, indicated in red, whilst the electrons move in the vacuum channel perpendicular to the laser traveling direction.

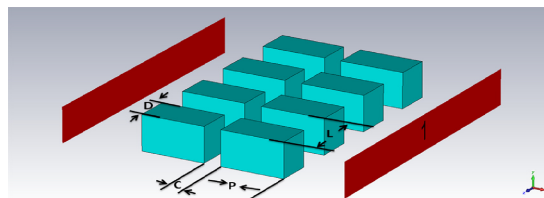


Figure 1: Structure dimensions, C represents the vacuum channel, P the pillar height, L the lattice constant and D the dielectric length.

As the laser light passes through the structure, the light speed in the grating pillar is lower than that in the adjacent vacuum space. This produces the desired π -phase-delay and a periodic electric field distribution inside the vacuum channel along the longitudinal beam axis. Figure 2 shows the z -component of the E -field, where the z -axis corresponds to the longitudinal beam direction. Along the vacuum channel, regions of the oscillating electric field of opposite polarity are spaced by $\lambda/2$.

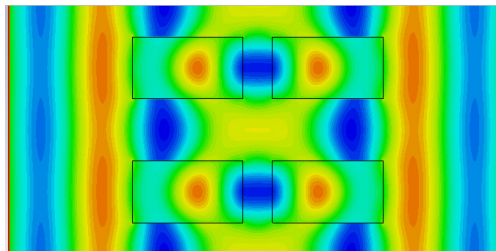


Figure 2: Electric field z -component peak distribution, colours represent field intensity and direction.

Consequently relativistic electrons catch up with the oscillating field which has a phase velocity equal to the speed of light in vacuum and are accelerated. The optimum pillar height and vacuum channel gap are determined in simulation studies. For the electric field calculation we used CST Microwave Studio. Figure 3 shows the electric field z -component peak distribution along the vacuum channel.

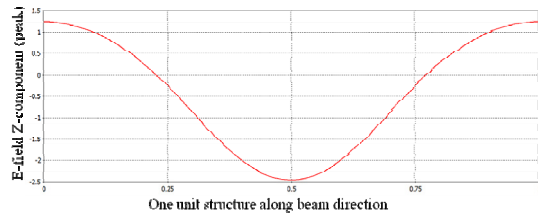


Figure 3: z-component of the electric field peak distribution along the vacuum channel.

Note that all structure lengths in this paper are normalized by the laser wavelength, and all field strengths are normalized by the laser amplitude. From this figure one can see that not only the phase is manipulated by the periodic structure, but also that the field amplitude is efficiently adjusted. Due to the diffraction effect, light is focused in the high refractive index region. Figure 4 shows that this mechanism of feeding the laser from two sides efficiently decreases the transverse field, i.e. the x-component which is perpendicular to the beam traveling direction and which is therefore unusable for longitudinal acceleration.

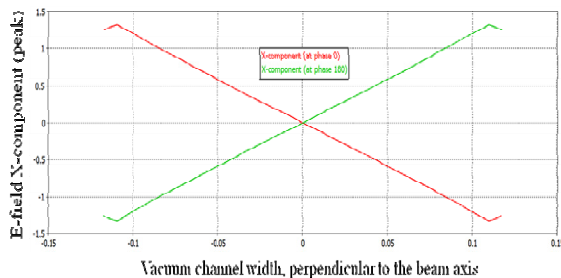


Figure 4: x-component of the electric field peak distribution along the x direction, perpendicular to the beam axis.

For the laser wavelength, we chose 1550 nm in all simulations, since many dielectric materials show high transparency at this wavelength. The final material for the accelerator structure is then chosen with respect to its transparency range, electric field damage threshold, thermal conductivity, nonlinear optical coefficients, chemical stability and refraction index. In all simulations, we selected silicon, which has an index of $n=1.527$ [6].

ACCELERATION GRADIENT AND LASER REQUIREMENTS

We have determined the acceleration field gradient by particle track simulation using CST Particle Studio. The resulting acceleration gradient is 3.2 GeV/m for an unloaded maximum field of 9.8 GV/m so that about 1/3 of the maximum electric field is converted into the average acceleration gradient. One of the advantages of dielectric laser accelerators is that the dielectric materials can sustain a higher electric field. For laser pulses below 1 ps the damage threshold of the dielectric grating structure has been measured to be ~ 2 J/cm² [7]. Figures 5 and 6 show the average acceleration gradient with different structure dimensions.

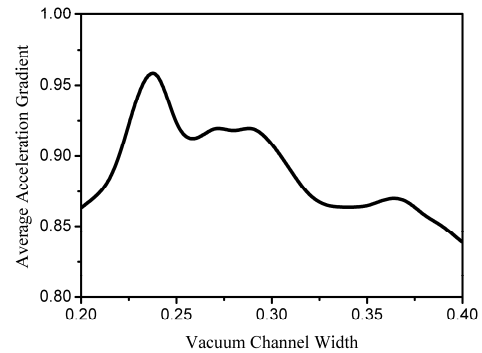


Figure 5: Relationship between normalized average acceleration gradient and vacuum channel width.

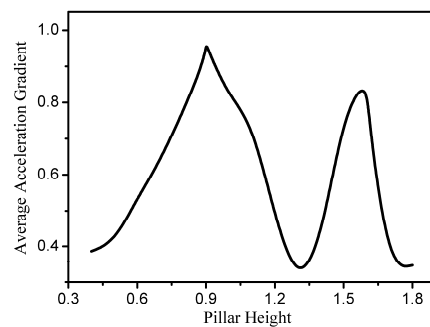


Figure 6: Normalized average acceleration gradient as a function of pillar height.

The optimum vacuum width is 0.24λ , and the optimum pillar height is 0.9λ . We have also analytically estimated the required laser parameters to feed a 10 mm-long structure from one side, and have listed the laser parameters in Table 1.

Table 1: Required Laser Parameters

Laser characteristics	Required parameters
Pulse energy	20 μ J
Average power	2 kW
Pulse width	100 fs
Repetition rate	100 MHz
Initial electron energy	30 MeV (relativistic)

It can be seen that fibre lasers are best selected as light source, due to their unique advantages in terms of compactness, stability, no need for cooling, high repetition rate and low cost.

The dual-grating accelerator structure is different from waveguide accelerator structures in that the electromagnetic wave travels perpendicular to the electron beam moving direction. Figures 7 and 8 show simulation results obtained with the Finite-Difference Time-Domain (FDTD) method.

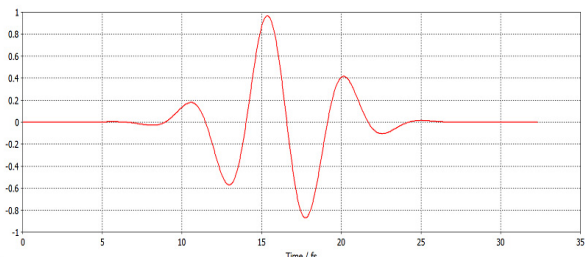


Figure 7: Normalized excitation signal, 10 fs plain wave, central wavelength of 1550 nm.

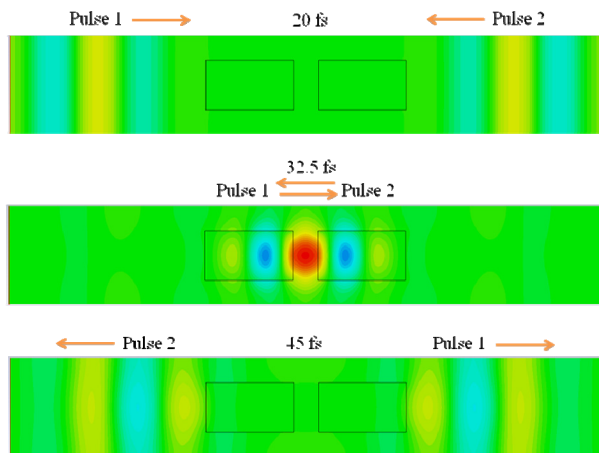


Figure 8: Illustration of electromagnetic wave propagation.

FUTURE PROSPECTS AND CHALLENGES

We propose a new structure which is expected to provide better beam confinement and simplify manufacture. Figure 9 explains the geometry of the structure. When electrons travel along the channel, the space charge effect scatters the beam. The charges collected on the wall then provide a Coulomb force on the beam which pushes the charges back to the axis. Figure 10 shows the electric field z-component peak distribution along the vacuum channel. In this case the wall thickness is 0.5λ , pillar height and vacuum channel width are chosen as 0.9λ and 0.24λ , respectively.

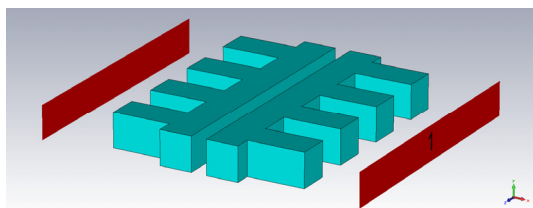


Figure 9: Dual-gratings accelerator structure with walls.

To pave the way for ultra-compact electron accelerators one needs to decrease the size of the injector. This can be achieved by using a compact 60 kV power supply which has recently become available [8]. The problem, however, is how to synchronize such low energy electrons with the fast changing electric field as the transit time of the

electrons along the period of the grating structure must be equal to the time-period of the laser light.

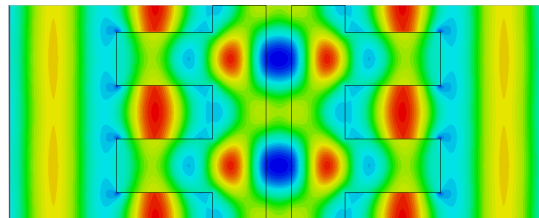


Figure 10: z-component of the E-field peak distribution.

This will require a multi-stage acceleration scheme. An optimized parameter set for the lattice constant of the grating and initial speed of the injected electrons is currently under investigation. It is planned to analyse beam loading in hundreds-nm-wide and few-cm-long vacuum cavities in a next step.

CONCLUSION

Dielectric laser accelerators are suitable for detailed investigations into the effects from radiation on biological cells. In this contribution we presented initial results on a single step dielectric laser acceleration experiment. We identified optimum grating parameters for the acceleration of relativistic electron beams. It was found that in this case the dual-grating lattice constant should equal to one laser wavelength, whilst pillar and vacuum length should be both equal to half the laser wavelength. The maximum acceleration field gradient appears when the pillar height and vacuum channel gap are equal to 0.9λ and 0.24λ laser wavelength, respectively. To accelerate lower energy particles it will be necessary to further adjust and optimize the structure dimensions.

REFERENCES

- [1] K. Koyama et al., “Designing of Photonic Crystal Accelerator for Radiation Biology”, Proc. IPAC, New Orleans, USA (2012).
- [2] T. Plettner, P.P. Lu, and R.L. Byer, “Proposed few-optical cycle laser-driven particle accelerator structure”, Phys. Rev. ST Accel. Beams 9, 111301 (2006).
- [3] X.E. Lin. “Photonic band gap fibre accelerator”, Phys. Rev. ST-AB 4 051301 (2001).
- [4] B.M. Cowan. “Three-dimensional dielectric photonic crystal structures for laser-driven acceleration”, Phys. Rev. STAB, 11:011301, 2008.
- [5] R.J. England et al., “Manufacture And Testing of Optical-Scale Accelerator Structures From Silicon And Silica”, Proc. IPAC, New Orleans, USA (2012).
- [6] G. Ghosh, “Dispersion-equation coefficients for the refractive index and birefringence of calcite and quartz crystals”, Opt. Commun. 163, 95-102 (1999).
- [7] K. Soong, R. L. Byer, C. McGuinness, E. Peeralta, E. Colby, and Menlo Park. “Experimental Determination of Damage Threshold Characteristics of IR Compatible Optical Materials”, Proc. PAC, New York City, USA (2011).
- [8] R. Suzuki, “Development of battery-operated portable high-energy X-ray sources”, Synthesiology-English edition, Vol.2 No.3, 221-228 (2009).